Water Resources Research

Key Points:
- The naturalized flow of the Colorado River has decreased about 15% over the last 100 years
- About half of the long-term trend is attributable to rising temperatures with the remainder due to changes in precipitation patterns and other factors
- Slightly over half of the flow reduction during the post-2000 Millennium Drought is attributable to anomalously warm temperatures

Supporting Information:
- Figure S1

Correspondence to:
D. P. Lettenmaier,
dlettenm@ucla.edu

On the Causes of Declining Colorado River Streamflows

Mu Xiao[1] (iD), **Bradley Udall[2]** (iD)**, and Dennis P. Lettenmaier[1]** (iD)

[1]Department of Geography, University of California, Los Angeles, CA, USA, [2]Colorado Water Institute, Colorado State University, Fort Collins, CO, USA

Abstract The Colorado River is the primary surface water resource in the rapidly growing U.S. Southwest. Over the period 1916–2014, the Upper Colorado River Basin naturalized streamflow declined by 16.5%, despite the fact that annual precipitation in the UCRB over that period increased slightly (+1.4%). In order to examine the causes of the runoff declines, we performed a set of experiments with the Variable Infiltration Capacity hydrology model. Our results show that the pervasive warming has reduced snowpacks and enhanced evapotranspiration over the last 100 years; over half (53%) of the long-term decreasing runoff trend is associated with the general warming. Negative winter precipitation trends have occurred in the handful of highly productive subbasins that account for over half of the streamflow at Lee's Ferry. We also compared a midcentury drought with the (ongoing) post-Millennium Drought and find that whereas the earlier drought was caused primarily by pervasive low-precipitation anomalies across UCRB, higher temperatures have played a large role in the post-Millennium Drought. The post-Millennium Drought has also been exacerbated by negative precipitation anomalies in several of the most productive headwater basins. Finally, we evaluate the UCRB April–July runoff forecast for 2017, which decreased dramatically as the runoff season progressed. We find that while late winter and spring 2017 was anomalously warm, the proximate cause of most of the forecast reduction was anomalous late winter and early spring dryness in UCRB, which followed exceptionally large (positive) early winter precipitation anomalies.

Plain Language Summary As the essential water resource for the Southwest United States, the Upper Colorado River Basin (UCRB) unimpaired streamflow declined by 16.5% over 1916–2014, while annual precipitation increased slightly (+1.4%). We performed a set of experiments with a hydrology model that uses temperature and precipitation as inputs to diagnose the causes of this apparent anomaly. We find that over half (53%) of the decreasing runoff trend is associated with unprecedented basin-wide warming, which has reduced snowpack and increased plant water use. The remaining ~47% of the trend is associated mostly with reduced winter precipitation in four highly productive subbasins, all located in Colorado. We compared the 1953–1967 drought with the 2000–2014 Millennium Drought and find that the earlier drought was caused primarily by precipitation declines across the entire UCRB but higher temperatures caused about half of the 2000–2014 flow loss. The Millennium Drought was also caused by precipitation reductions in the four most productive subbasins. We evaluated the UCRB April–July runoff forecast for 2017, which decreased dramatically as the runoff season progressed. The late winter and spring 2017 was anomalously warm, but most of the reduction was due to late season dryness.

1. Introduction

The Colorado River is the largest river in the southwestern U.S. It is the source of drinking water for many of the Colorado River Basin's 40 million people and provides irrigation water to ~13,000 km^2 of crops in the U.S. and Mexico (Cohen et al., 2013). It is a lifeline for the population and agricultural economy of parts of seven U.S. states (WY, UT, CO, NV, NM, AZ, and CA) and the Mexican states of Sonora and Baja California. The river's naturalized streamflow (see section 2.2 for discussion of naturalized streamflows) at Imperial Dam (the downstreammost long-term gauging station) has averaged about 20.7 km^3/yr (16.8 maf/yr) over the last century, approximately 90% of which is generated in the Upper Colorado River Basin (McCabe & Wolock, 2007), defined as the ~289,000 km^2 of drainage area upstream of the U.S. Geological Survey stream gauge at Lees Ferry, AZ (USGS 09380000). Snowpack stored in the high-elevation Rocky Mountain headwater basins contributes about 70% of the annual streamflow (Christensen et al., 2004).

The Colorado River is heavily regulated, mostly by Glen Canyon Dam (Lake Powell) and Hoover Dam (Lake Mead), with combined reservoir storage capacity of 67.5 km^2 (54.7 maf). The importance of these

reservoirs, which can store close to 4 times the natural annual flow at Lees Ferry, AZ, has become especially evident during the so-called Millennium Drought, which began about 2000. This drought has coincided with increases in water demand (Rajagopalan et al., 2009), which resulted in Lake Mead reaching its lowest level on record in October 2016. Lakes Mead and Powell dropped precipitously from 2000 to 2004 due to very low flows (71%, 74%, 41%, 71%, and 64% of average, respectively) and have not recovered due to continued high demands equal to inflows and a lack of high flow years. Indeed, only four of the last 18 years have had above average river discharge, limiting reservoir refill opportunities.

A pronounced warming trend across the Colorado River Basin (CRB) since the 1970s (Dawadi & Ahmad, 2012) has further contributed to the post-2000 imbalance between CRB runoff and water demand. Vano et al. (2012) evaluated the temperature sensitivity (annual average streamflow change per 1 °C temperature change) and found that the average sensitivity of annual runoff at Lees Ferry was around −5%/°C), suggesting that warming over the last ~50 years may account for a 5–10% reduction in annual streamflow over that period.

Several studies have investigated the effects of ongoing warming on the flow of the Colorado River. Barnett and Pierce (2009) concluded that anthropogenic climate change would reduce CRB runoff by 10%–30% by 2050. Reynolds et al. (2015) predicted that minimum streamflows will decline as warming of the basin continues. Woodhouse et al. (2016) reported an increase in the frequency of warm years with low streamflow since 1988. McCabe et al. (2017) found that increases in temperature since the late 1980s have decreased runoff generation efficiency, reducing streamflows by 7%. Udall and Overpeck (2017) similarly found temperature-induced streamflow decreases of approximately 6% during 2000–2014 and projected large midcentury temperature-induced declines of 20% or more should precipitation not change.

Here we utilize a hydrological model applied for the period 1916–2014 (all data are for water years if not specified otherwise) to evaluate the spatial and temporal signature of the Millennium Drought in the CRB. Along with a baseline simulation forced by gridded observations, we perform a T-detrend experiment, in which we remove the long-term temperature trend from the model forcings, to investigate the role of the warming on streamflow declines both over the long term and during the recent drought. We analyze runoff in each of 20 subbasins of the CRB, which allows us to study spatial variations in runoff generation and anomalies. We also analyze the historical 1953–1968 drought in an attempt to shed light on how the hydrologic response to climate variations has changed in recent decades and during the Millennium Drought in particular. Finally, we dissect the 2017 April–July streamflow forecast to understand the role of late winter and early spring precipitation and temperature in the substantial seasonal forecast reductions that occurred as water year 2017 progressed.

2. Data and Approach

2.1. VIC Model and Forcings

The Variable Infiltration Capacity (VIC) model is a physically based, semidistributed hydrological model, which represents the land surface water and energy budgets over a grid mesh (here 1/16th degree spatial resolution) and routes runoff through a prescribed river network to produce streamflow estimates at specified river nodes (Liang &Lettenmaier, 1994). We applied the model at a daily time step, using what is termed full-energy balance mode, meaning that the model iteratively solves the surface energy budget by estimating the effective surface temperature at each time step. Therefore, the daily average surface temperature produced by VIC is not the average of the forcing temperatures, that is, 0.5*(daily maximum + daily minimum). Unless stated otherwise, the temperatures we report here are outputs from the VIC simulations.

Similar to other land surface models, the fundamental water balance equation in VIC can be summarized as Runoff (RO) = Precipitation (P) − Evapotranspiration (ET) − changes in Soil Moisture (ΔSM) − changes in Snow Water Equivalent (ΔSWE). Groundwater is not represented in the version of VIC we used; Rosenberg et al. (2013) found that inclusion of a parameterization of groundwater had little effect on the model's streamflow simulations in the CRB. It is important to note that VIC represents snowpack sublimation within its winter ET. Sublimation is sparsely measured but nonetheless is important to some aspects of our study (Andreadis et al., 2009); we describe the model's performance with respect to sublimation in section 4.2.
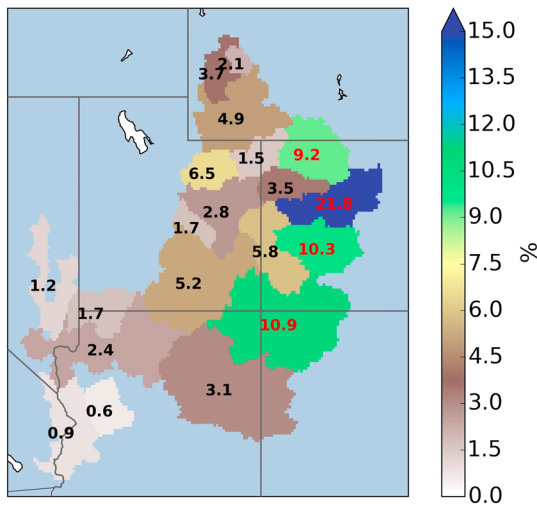
Figure 1. Percent of total CRB runoff (at Imperial Dam) originating from 20 subbasins, calculated based on long-term average from VIC simulation for water years 1971–2014. The subbasins shown in Figure 1 were extracted from a published data set by Wu et al. (2012).

The VIC model has been successfully applied previously in a number of hydrological studies over the CRB and the U.S. Southwest (Christensen et al., 2004; Christensen & Lettenmaier, 2007; Mote et al., 2005, 2018; Vano et al., 2012, 2014).

The VIC model simulates surface hydrological processes with parameterizations of subgrid vegetation, soil variability, and topography and has provided plausible representations of CRB surface water conditions in the above-referenced studies. We forced the model with an updated version of the Hamlet and Lettenmaier (hereafter H&L) data set (Hamlet & Lettenmaier, 2005) at 1/16° resolution for the period water years 1916–2014. We chose the H&L data set because its long-term variability is indexed to the U.S. Historical Climatology Network (HCN; Easterling et al., 1996) stations in the region, which have been carefully quality controlled for effects that could otherwise result in spurious trends, such as station moves and instrument changes (e.g., the shift to maximum-minimum temperature system temperature sensors in the 1980s). As described in Hamlet and Lettenmaier (2005), the H&L data set uses HCN station data to constrain decadal variability (and hence long-term trends), hence is in our view most appropriate for exploration of the causes of century-scale streamflow declines over our study period 1916–2014.

2.2. Naturalized Streamflows

To evaluate our model simulation results, we used naturalized streamflow data for the Colorado River produced by the U.S. Bureau of Reclamation (USBR); see https://www.usbr.gov/lc/region/g4000/NaturalFlow/current.html for details. The naturalized streamflows are derived from USGS historical streamflow observations by a process of adjustments that compensate for anthropogenic effects including consumptive uses of water, reservoir storage, transbasin diversions, and other effects (see USBR, 1983). The naturalized streamflow data sets are produced for 29 well-distributed tributary stations across the CRB (as well as the main stem) for the period 1906 through 2015. Others (Prairie & Callejo, 2005) have noted that USBR has improved the quality of the naturalized flow data set after 1971 and the estimates may be somewhat better after that time.

2.3. Subbasin Analysis

We performed our analyses for the Colorado River above Imperial Dam, as well as for the 20 subbasins delimited by USGS WaterWatchgauges (see Figure 1), which are a subset of the 29 naturalized streamflow points noted above. The river channel network data set we used is from Wu et al. (2012), based on which we determined the masks for each of the 20 subbasins. The Wu et al. subbasins are similar to, but slightly different from, the more familiar six-digit Hydrologic Unit Codes normally used in the basin. Detailed information about each subbasin is reported in the supporting information.

It is important to note that our analysis excludes the Gila River given its distinct hydrological and legal characteristics. The Gila River joins the Colorado River below Imperial Dam just upstream of the U.S. border with Mexico and in recent years has been mostly dry at its mouth due to upstream uses by Arizona. Since 1964, the U.S. Supreme Court has excluded it from administration under the Colorado River Compact. Although the Gila is an important basin, its absence from this study is logical given its unique status.

2.4. Model Testing and Evaluation

Table 1 summarizes the long-term runoff contribution percentages from nine major subbasins at which naturalized streamflows are available and for which we also produced VIC simulations. The runoff contribution percentages from the model and naturalized flows generally are in good agreement. The Upper Basin (UCRB; defined as the drainage area above

Table 1

Naturalized (NFL) and VIC Runoff Contribution Percentages for Selected USGS Gauges

Station name	NFL	VIC
COLORADO RIVER NEAR CAMEO (09095500)	22.8%	21.8%
GUNNISON RIVER NEAR GRAND JUNCTION (09152500)	14.6%	10.3%
SAN JUAN RIVER NEAR BLUFF (09379500)	12.4%	10.9%
GREEN RIVER NEAR GREENDALE (09234500)	12.2%	10.7%
WHITE RIVER NEAR WATSON (09306500)	3.5%	3.5%
DUCHESNE RIVER NEAR RANDLETT (09302000)	4.8%	6.5%
YAMPA RIVER AT DEERLODGE PARK (09260050)	8.0%	9.2%
COLORADO RIVER AT LEES FERRY LEEFY (09380000)	91.8%	91.0%
COLORADO RIVER ABOVE IMPERIAL DAM (09429490)	100%	100%

Note. Values are computed relative to the annual streamflow climatology at the Imperial Dam, AZ-CA. The percentages are relative to long-term averages for water year 1971–2014.
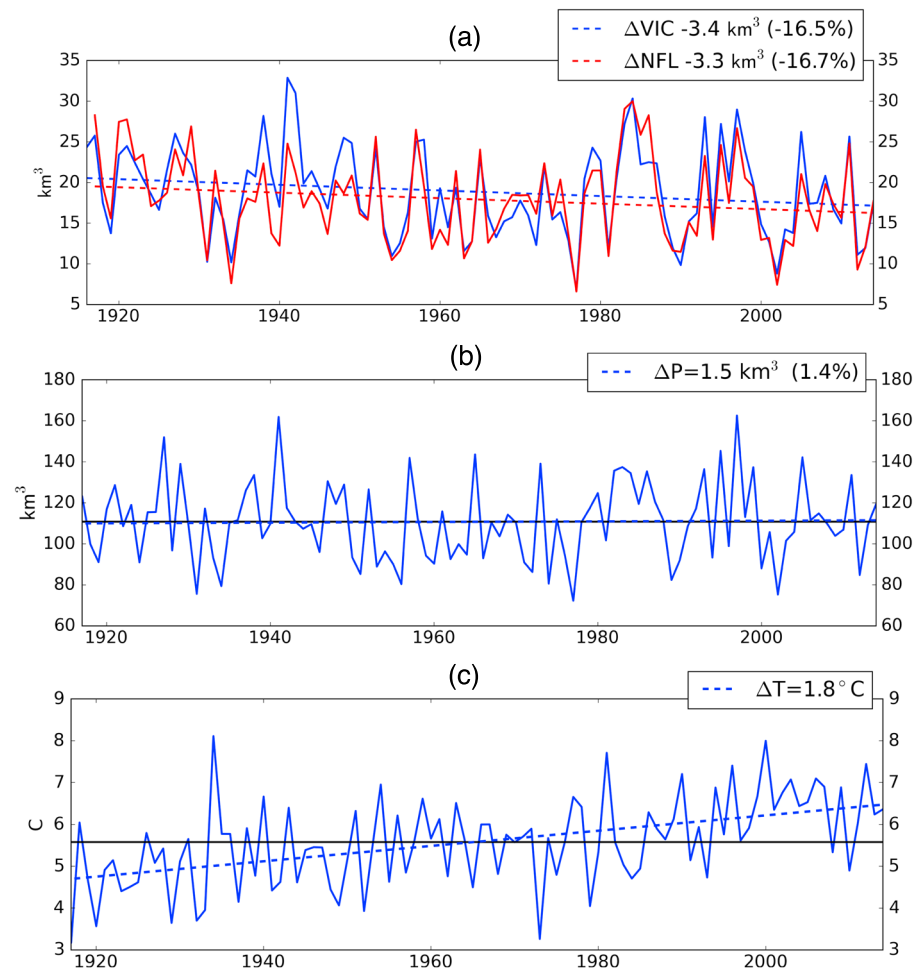
Figure 2. Annual time series and linear regression trend plots for Colorado River Basin above Lees Ferry: (a) annual (naturalized) runoff, (b) annual precipitation, and (c) annual average surface temperature calculated by VIC. Changes are calculated relative to the starting value of the fit. Note that precipitation (b) is from an extended version of the Hamlet and Lettenmaier (2005) data set at 1/16th degree spatial resolution, while temperature (c) is calculated from VIC and is approximately 0.4 °C warmer than the Hamlet and Lettenmaier input temperature.

Lees Ferry, AZ) produces more than 90% of the flow at Imperial Dam. Therefore, we mainly focus on the UCRB here, acknowledging unusual Lower Basin (LCRB) conditions when noteworthy.

Figure 2a shows the annual time series of naturalized streamflow (NFL) and VIC simulations at Lees Ferry, AZ. Both the annual naturalized streamflows and VIC simulations ($r^2 = 0.75$) and their trends over the period of record (NFL: -3.3 km^3/yr, VIC: -3.4 km^3/yr) are similar, suggesting that the VIC model provides a plausible representation of natural conditions (i.e., those responding primarily to climate forcings) and long-term hydrologic change in the basin. Hereafter, we mainly focus on VIC results in our analysis of UCRB subbasin long-term (1916–2014) trends and comparison between the 1953–1968 and the Millennium drought. The annual precipitation and average temperature (calculated by VIC as noted in section 2.1) time series plots are also presented in Figure 2.

3. Results

3.1. Basin-Wide Trend Analysis

Table 2 summarizes long-term linear (regression) trends for the UCRB for four hydrological variables (precipitation, evapotranspiration, runoff, and 1 April snow water equivalent) from the baseline VIC simulation and the temperature-detrended (T-detrend) simulation. We also computed trends using the

Table 2
UCRB Annual and Seasonal Changes in Water Balance Variables Over Water Years 1916–2014 in km^3/yr (km^3 for SWE) and Percentages Relative to the Starting Value of the Fit

	P	T	ET	ET-D	RO	RO-D	SWE	SWE-D
Annual	1.5 (1.4%)	1.8	4.2 (4.7%)	2.3 (2.6%)	−3.4 (−16.5%)	−1.6 (−7.7%)	−9.1 (−39.0%)	−5.6 (−23.9%)
Winter	−0.1 (−0.2%)	1.9	4.9 (30.5%)	2.9 (18.0%)	0.4 (10.4%)	0.4 (9.0%)	Na	Na
Summer	1.6 (3.0%)	1.7	−0.8 (−1.1%)	−0.6 (−0.8%)	−3.8 (−23.3%)	−1.9 (−11.9%)	Na	Na

Note. P is precipitation, T is temperature in Celsius, ET is evapotranspiration, RO is total runoff, and SWE is 1 April snow water equivalent. Dashed "D" denotes results from T-detrend simulation. Winter period is October–March, and summer period is April–September.

nonparametric Theil-Sen slope estimator (Sen, 1968; Theil, 1950) and found that they generally are in close agreement (Table S1). Therefore, we refer to the linear trends hereafter for convenience. The T-detrend simulation uses the same forcings as the baseline, except that annual linear trends in the daily temperature maxima and minima are removed. We also disaggregated summer season (April–September) and winter season (October–March) for each variable (all summers and winters mentioned hereafter are so defined).

Over the simulation period 1916–2014 the UCRB annual precipitation increased by +1.5 km^3 (1.4%), whereas winter precipitation, which is the main source for 1st April snow water equivalent and streamflow in the spring and summer, had only a very small (not statistically significant) negative trend (long-term ΔP is −0.1 km^3, −0.2%). In our baseline simulation, the long-term linear change of annual runoff (ΔRO) in the UCRB is −3.4 km^3 (−16.5%) and long-term change in annual evapotranspiration (ΔET) is +4.2 km^3 (+4.7%). The 1st April SWE decreased significantly (ΔSWE −9.1 km^3, −39.0%), which reduces warm season streamflow from the Upper Basin, as evidenced by summer RO decreases (−3.8 km^3, −23.3%) even given a positive trend in summer precipitation (ΔP_{summer} is +1.6 km^3). As summer RO makes up more than 3/4 of the annual RO in the UCRB, the long-term annual ΔRO is negative as noted above, although summer RO decreases are slightly compensated by increasing winter RO (ΔRO_{winter} + 0.4 km^3, 10.4%).

We performed the T-detrend simulation using the same precipitation as the baseline simulation but with the temperature trend removed from the forcing data set on a grid cell by grid cell basis. In this no-warming-trend scenario, the long-term decreasing trend in annual runoff is reduced to −1.6 km^3 (−7.7%), from −3.4 km^3 but not eliminated. It suggests that 53% (−1.8/ −3.4) of the annual runoff trend is attributable to the annual warming temperature. The increase in ET in the T-detrend simulation is smaller by 1.9 km^3 (baseline: +4.2 km^3, T-detrend: +2.3 km^3), which explains the increase in runoff (1.8 km^3) to within 0.1 km^3.

The numbers in Table 2 also show that the effects of the temperature trend on winter RO (baseline: +0.4 km^3, T-detrend: +0.4 km^3) and summer ET (baseline: −0.8 km^3, T-detrend: −0.6 km^3) are small. Increasing temperatures cause a decrease in summer RO (baseline: −3.8 km^3, T-detrend: −1.9 km^3) and an increase in annual ET (baseline: +4.2 km^3, T-detrend: +2.3 km^3) that comes mostly in the winter (baseline: +4.9 km^3, T-detrend: +2.9 km^3). On a percentage basis, both of these increasing winter trends in ET are substantial over the 1906–2014 period: a 30% increase in the baseline ET and an 18% increase in the T-detrend simulation ET. The summer ET changes of −1.1% and −0.8% are comparatively small. It is worth noting that the long-term trend in UCRB winter ET is positive in the T-detrend simulation even given no significant trend in winter precipitation. The positive trend in winter ET is mainly caused by increased snow sublimation. Although sublimation is strongly controlled by surface temperature, other factors also contribute as well (see section 4).

The remaining −1.6 km^3 (−7.7%) decrease in RO in the T-detrend simulation is curious given the increasing summer precipitation (ΔP_{summer} + 1.6 km^3, 3.0%) and negligible winter precipitation change (ΔP_{winter} − 0.1 km^3, −0.2%). In addition, although the SWE anomaly in the T-detrend simulation is less compared with that of the baseline simulation (baseline: −9.1 km^3, T-detrend: −5.6 km^3), the long-term 1906–2014 SWE trend is still negative in the T-detrend simulation (−23.9%). Winter ΔET in the T-detrend simulation is only +2.9 km^3 as reported in Table 2, which cannot explain all of the SWE anomaly. One possible answer is that while the overall basin-wide precipitation changes over time are small, precipitation declines in the most productive basins while increasing in the less productive basins. We explore the effects of such spatial variations below.
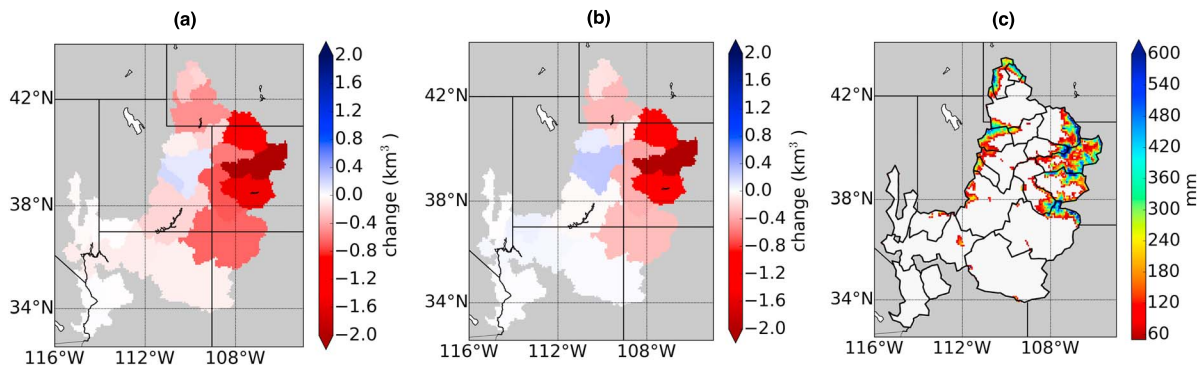
Figure 3. Spatial plots of 1 April SWE trends for (a) baseline simulation and (b) T-detrend simulation over each subbasin. The changes over 1916–2014 are calculated relative to starting value of the linear regressions. (c) Long-term average 1 April SWE.

3.2. Subbasin Conditions

Figure 1 shows that there are four subbasins in the upper CRB (denoted by red numbers) that produce most of the UCRB runoff: the Yampa River, Colorado River near Cameo, Gunnison River, and San Juan River (from north to south, respectively). The most productive subbasin is the Colorado River near Cameo (USGS 09095500) in the northeastern part of the UCRB. This subbasin produces almost one quarter of the total naturalized runoff of the UCRB. It contains not only the mainstem but also several large tributaries, including the Eagle, the Roaring Fork, and the Blue. A little more than 30% of the UCRB flow is produced by the other three subbasins, and in total, about 55.5% of the total discharge of the UCRB is attributable to these four tributaries. Below, we discuss the nature of the long-term changes in these critical subbasins.

Figure 4 shows annual precipitation, ET, and runoff changes for all subbasins over the 1916–2014 study period. The top row is extracted from our baseline simulation, and the bottom row is from the T-detrend simulation. We note that although some subbasins appear similar between baseline and original maps, the
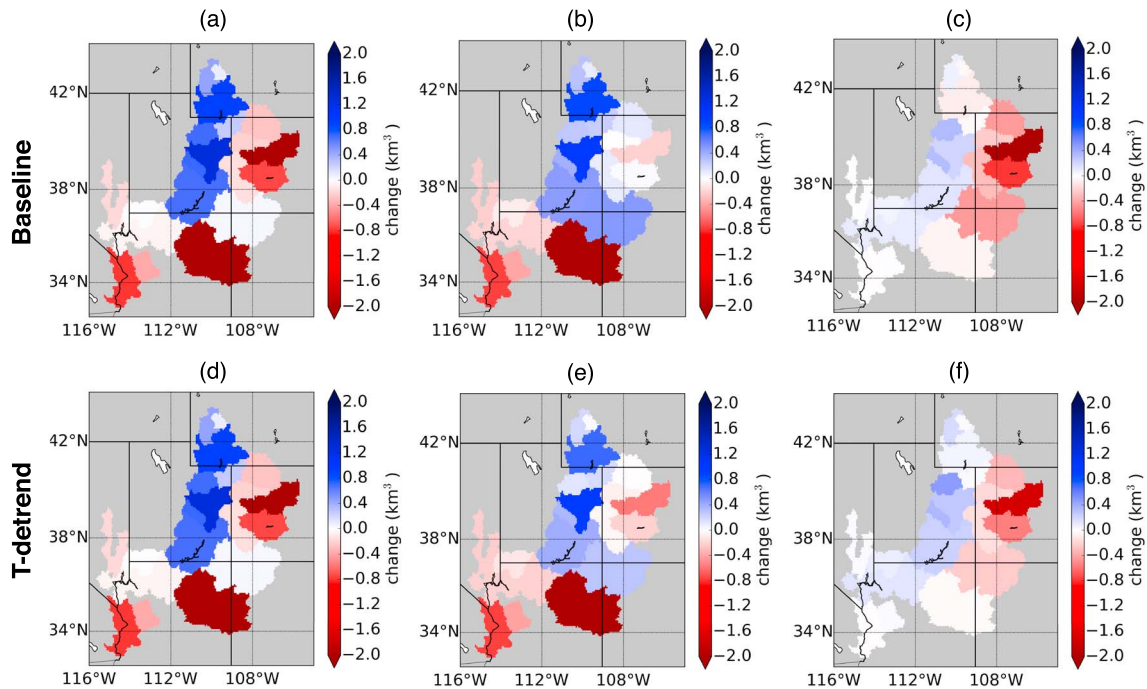

Figure 4. Spatial changes of (a) annual precipitation from gridded observations, (b) ET, and (c) runoff from baseline VIC simulation over 1916–2014 for CRB above Imperial Dam. Changes are calculated relative to the starting value of linear fits. Panels (d)–(f) are the same as (a)–(c), but variables are extracted from the T-detrend simulation. Panels (a) and (d) are identical.
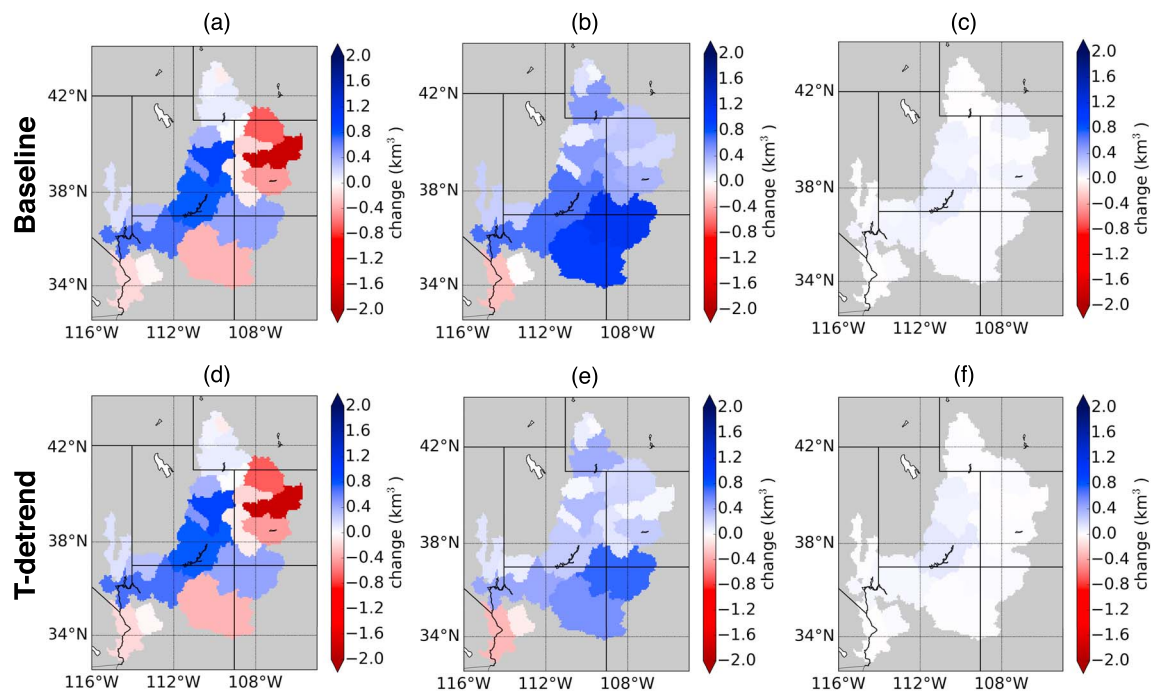
Figure 5. Same as Figure 4 but for winter (October–March).

numbers are more different than they might appear by visual inspection of the maps (Tables S3 and S4). We calculated the changes relative to the initial value of each linear fit, shown in Table 2. Figure 4a shows a note-worthy east-west dipole in the precipitation changes over time in the UCRB. In the UCRB, precipitation decreases have occurred mainly in the high runoff generating northeastern part of the basin, while several subbasins in the northwestern part of UCRB show long-term annual precipitation increases.

Precipitation declines have also occurred in the LCRB where little runoff occurs. These decreases in precipitation led to declines in ET and little change in subbasin runoff (Figures 4c and 4f), with negligible impact on total basin runoff (e.g., at Imperial Dam).

There are two subbasins in the northeastern part of the UCRB, which have relatively large annual precipitation decreases of -2.3 km^3 (Colorado River above Cameo) and -0.7 km^3 (Gunnison River) with a combined runoff decrease of -2.9 km^3 (supporting information). These are the same highly productive subbasins shown in Figure 1 and are a major driver of the overall annual runoff decline. Four basins in the northwestern part of UCRB with increasing precipitation (the Green River downstream portion along with its San Rafael River and Duchesne River tributaries; colored in deeper blues in Figure 4) have partially offset these long-term runoff declines by about 1.0 km^3.

Figures 5 and 6 are similar to Figure 4 but for winter (October–March) and summer (April–September), respectively. Winter runoff changes are small for both the baseline and T-detrend simulations, as most runoff occurs during the summer season. Although the total precipitation amounts are similar during warm and cold seasons, winter precipitation is much more important to the UCRB's runoff. Summer precipitation mainly contributes to ET rather than runoff, as high summer temperatures lead to large ET, especially at lower elevations. Winter precipitation in mountain headwater regions accumulates as snowpack and contributes mostly to RO rather than ET, when it melts.

The 1 April SWE trend plots for all the subbasins (Figures 3a and 3b) show that the four highly productive subbasins (Yampa River, Colorado River near Cameo, Gunnison River, and San Juan River) in the northeastern part of the basin that contribute much of the runoff losses in the UCRB have all experienced substantial SWE decreases. Those subbasins are also snow-dominant regions as indicated by Figure 3c. Figure 5a shows that winter precipitation has declined in all of the northeast UCRB subbasins except for the San Juan River, which shows a positive winter precipitation trend. Nonetheless, both SWE (Figure 3a) and annual RO (Figure 4c) in
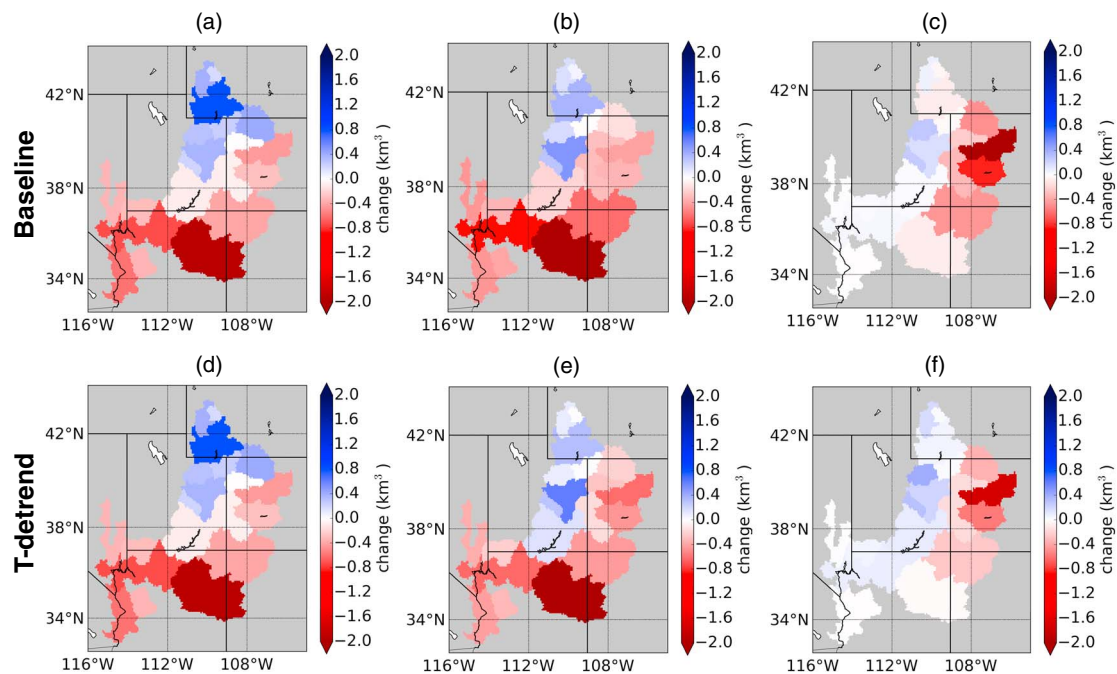
Figure 6. Same as Figure 4 but for summer (April–September).

the San Juan Basin are decreasing. The reason is that winter ET has increased substantially: ΔP_{winter} is +0.4 km^3, while long-term ΔET_{winter} is +1.1 km^3, with SWE decreasing by −0.7 km^3, or −30.1%. Declines in SWE in the other three basins, all of which experience declines in precipitation, are more severe and range from −46% to −49%. The increased winter ET, along with reductions in precipitation in these basins, explains the strongly decreasing SWE and substantially explain the declines in subbasin runoff.

As noted above, 53% (1.8 of 3.4) of the long-term runoff trend in the UCRB is related to warming temperatures. To dissect the remaining −1.6 km^3 (−47%) in the T-detrend simulation, we performed a P- and T-detrend experiment, in which we removed both the temperature and winter precipitation trend from the original input data set. Importantly, under this experiment the northeast UCRB basins see increased winter precipitation, while the northwest basins see decreased winter precipitation relative to the baseline and T-detrend simulations. Note, also, that we do not modify the summer precipitation, which increased over the study period. Under the P&T-detrend simulation, the UCRB's long-term runoff losses become −0.6 km^3 (1.0 km^3 less than the pure T-detrend and 2.8 km^3 less than the baseline). The residual −0.6 km^3 loss over the 1916–2014 period is attributable to increased winter ET. Section 4.2 below evaluates why ET_{winter} shows a positive trend given no P trend and no T trend. The total runoff decline of −3.4 km^3 can thus be attributed to warming (−1.8 km^3), insufficient P in the northeast part of CRB (−1.0 km^3), and increased winter ET (−0.6 km^3).

Summer precipitation and summer ET trend spatial plots (Figures 6a and 6d versus 6b and 6e) show similar patterns for both the baseline and T-detrend simulations: negative trends have occurred over the LCRB and the eastern UCRB, while some increases have occurred in the northwestern headwaters. The spatial patterns confirm that in the summer increases in precipitation drive increases in ET, while decreases in precipitation drive decreases in ET over both the LCRB and UCRB when surface air temperatures are relatively high.

In the UCRB the baseline simulation April–September runoff (Figure 6c), which constitutes almost three quarters of the CRB annual total, shows spatial patterns similar to the SWE spatial plots in Figure 3. Taken together, the figures show where water is stored as snow in the UCRB during winter in the cold, high-elevation headwater regions and how SWE then contributes to runoff in the following spring and summer. Over the last century, warming temperatures, reduced winter precipitation in the most productive mountain subbasins in the UCRB, and slight increases in winter ET (Figure 5b) lead to reduced SWE and consequently reduced runoff.
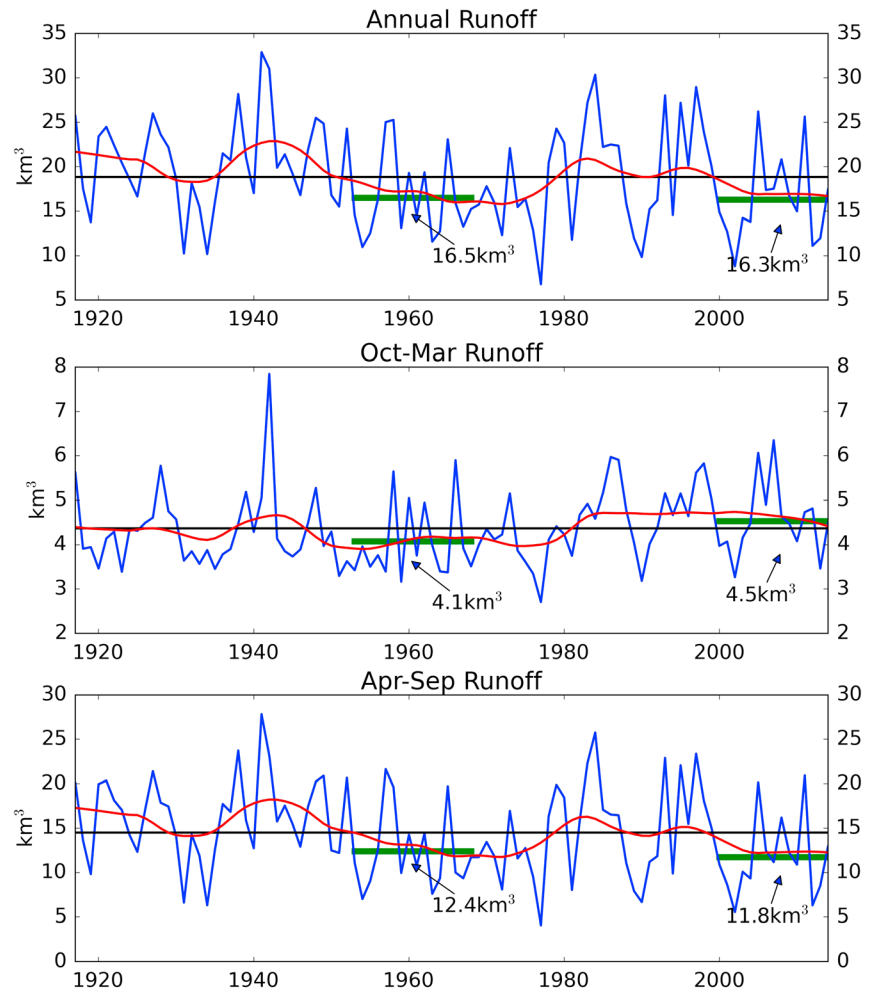
Figure 7. Time series of VIC simulations of annual runoff (top), winter runoff (middle), and summer runoff (bottom) at Lees Ferry (UCRB). The black horizontal lines are the long-term means, and red lines result from LOWESS filtering of VIC results.

In the LCRB, the annual precipitation, ET, and runoff plots show mostly P decreases, ET increases, and small RO changes (Figure 4). In winter, some P increases occur in the NW portion, ET increases everywhere except in the south, and RO has little change (Figure 5). Summer shows decreasing P, increasing ET, and little RO change (Figure 6).

3.3. Drought Comparisons

In order to examine the causes of the Millennium Drought, we compare the recent dry period from 2000 to 2014 (D2) with the 1953–1968 drought (D1). Figure 7 shows the time series of UCRB annual streamflow volume. Long-term averages are marked as the black horizontal baseline, and the Locally Weighted Scatterplot Smoothing (LOWESS) VIC streamflows are plotted in red. We report basin-wide (CRB, UCRB, and LCRB) annual average anomalies for four selected variables (P, SWE, ET, and RO) over the two drought periods in Table 3. Spatial anomaly plots by subbasin of P, SWE, ET, and RO for the 1953–1968 and 2000–2014 periods are shown in Figures 8 and 9.

Similar to the long-term trends discussed in section 3.3, comparison of the annual anomalies of precipitation, ET, and runoff during both droughts in Table 3 confirms that the UCRB dominates total basin-wide runoff production during drought periods as in the long term. In the Millennium Drought annual precipitation decreased more in the LCRB, which substantially reduced ET, but not runoff. This is a very large part of the overall basin-wide ET loss ($-7.9/-8.7$ km^3), but the LCRB ET does not make much difference to streamflow because most Lower Basin precipitation is converted to ET, drought or no drought. Since our primary interest is on the causes of declining runoff, we again focus on the UCRB.

AGU
100
ADVANCING EARTH
AND SPACE SCIENCE

Water Resources Research

10.1029/2018WR023153

Table 3
Annual Average Anomalies During the Midcentury Drought D1 (1953–1968) and Millennium Drought D2 (2000–2014) for CRB, UCRB, and LCRB

	P anomaly	P climatology	SWE anomaly	SWE climatology	ET anomaly	ET climatology	RO anomaly	RO climatology	T anomaly	T climatology
CRB-D1	−8.8	163.8	−2.9	19.3	−6.0	143.0	−2.7	20.7	0.0	8.5
CRB-D2	−11.4		−4.8		−8.7		−2.8		1.0	
UCRB-D1	−6.1	110.8	−2.7	18.7	−3.7	91.9	−2.4	18.9	0.1	5.6
UCRB-D2	−3.2		−4.4		−0.8		−2.6		1.0	
LCRB-D1	−2.7	53.0	−0.2	0.6	−2.3	51.1	−0.3	1.8	−0.2	13.0
LCRB-D2	−8.2		−0.4		−7.9		−0.2		1.0	

Note. Long-term climatologies are also provided. Results are relative to the 1916–2014 baseline simulation (Table 2); units are km^3 (except temperature is Celsius). The climatologies are extracted from the baseline simulation. (Table S6 includes the summer and winter anomalies for UCRB.)

Table 3 summarizes climate and hydrological differences and similarities between the two drought periods. In particular, UCRB RO anomalies for the two drought periods are quite similar (−2.4 versus −2.6 km^3; all the numbers are D1 versus D2 in this paragraph), whereas the SWE decrease is much greater in the Millennium Drought (−2.7 versus −4.4 km^3). Although the basin-wide annual (negative) precipitation anomaly in 1953–1968 is much less than the Millennium Drought (−8.8 versus −11.4 km^3), this order is reversed in the UCRB (−6.1 versus −3.2 km^3), where most runoff is generated. In the UCRB, the earlier 1953–1968 drought has less average annual precipitation than the Millennium Drought (104.6 versus 107.5 km^3), especially in winter when precipitation in the UCRB differentially contributes to runoff production, as discussed in section 3.2. Winter precipitation in the UCRB is 51.5 and 54.5 km^3 for 1953–1968 and 2000–2014, respectively, whereas summer precipitation is nearly identical (53.1 and 53.0 km^3; Table S6). Much higher temperatures (+0.1 versus +1.0 °C), less SWE (−2.7 versus −4.4 km^3), and more winter ET (+0.4 versus +1.8 km^3) are indicative of additional key differences between the two droughts.
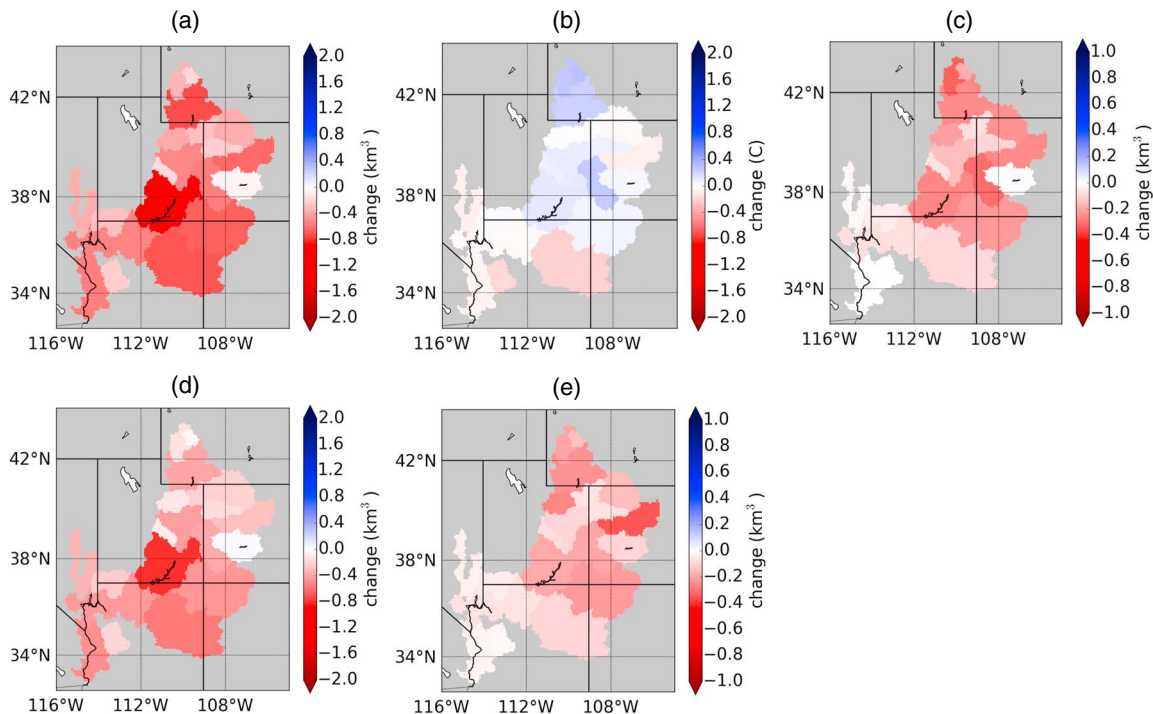

Figure 8. Average annual anomaly plots for each subbasin during the drought period 1953–1968. The variables in each panel are (a) precipitation, (b) temperature, (c) SWE, (d) ET, and (e) runoff (panels (c)–(e) are from VIC simulations).
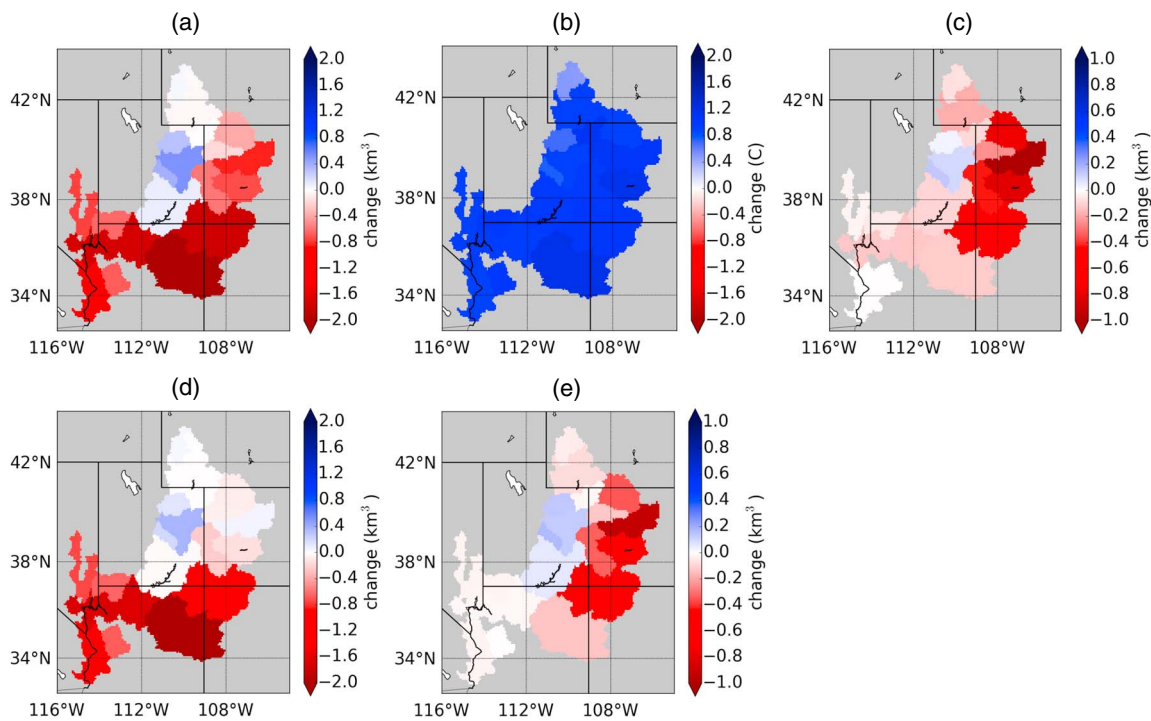
Figure 9. Same as Figure 8 but for 2000–2014 Millennium Drought.

Table 3 combined with Figures 8a–8e shows that the 1953–1968 drought mainly resulted from a spatially widespread and consistent negative precipitation anomaly across most of the UCRB. Temperatures were within 0.1 °C of the climatological mean. The corresponding ET and runoff anomalies therefore mostly reflect the precipitation reductions in each subbasin. SWE clearly decreases uniformly in almost all parts of the UCRB, as does runoff. Note that Figures 8a and 8c–8e all have similar patterns.

Interpretation of anomalies during the Millennium Drought is more complicated due to spatially heterogeneous conditions. Pervasive anomalously high temperatures, resulting in part from the long-term warming trend, which emerged around the 1970s and exacerbated by drought-specific warming, play a substantial role (Figure 9b). In addition, D2 average ET in the UCRB (Table 3 and Figure 9d), only 0.8 km^3 less than the climatological mean (despite drier conditions), combined with precipitation reductions in the most highly productive subbasins (Figure 9a) caused large runoff reductions in those key basins. In the UCRB, the western subbasins experienced positive precipitation anomalies with commensurate increases in ET. The northeastern subbasins where snow dominates and most of the UCRB runoff originates (Figure 3c) experienced negative precipitation anomalies but without commensurate decreases in ET, which acted to amplify the SWE reductions. Thus, Figures 9c and 9e show substantial declines in SWE and RO from these northeastern basins along with smaller declines and even some increases in SWE and RO from the northwestern basins. Unlike the 1950s drought, the spatial patterns in Figures 9a and 9c-e are highly complex.

Eight basins—four from the highly productive northeast and four from the less productive northwest—provide additional insights into how spatially heterogenous precipitation, ET, and SWE combined to produce spatially variable runoff in the Millennium drought. The four most highly productive sub-basins (marked with red numbers in Figure 1) contributed more than 83% of the total −2.6-km^3/yr RO anomaly in the Millennium Drought; their contribution was only 34% of the −2.4-km^3/yr RO anomaly during 1953–1968 (numbers of each subbasin are provided in the supporting information). Four subbasins on the western side of the UCRB (draining the Uinta and Central Utah Mountains) had positive annual precipitation anomalies during 2000–2014 (leading to 0.5-km^3/yr positive RO anomaly), but that positive anomaly was more than canceled by other runoff-losing subbasins (−2.4 km^3 for the four highly productive northeastern basins). Compared with 1953–1968, precipitation anomalies were much more uneven in the Millennium Drought. The

relatively evenly distributed positive +1 °C temperature anomalies lead to more winter ET (+0.8 km^3, 3.7% of the annual streamflow) and reduced SWE (−4.8 km^3, 23.0% of the annual streamflow), exacerbating the precipitation reductions over the UCRB.

By combining our T-detrend and P&T-detrend simulations, we can gain additional insights into the Millennium Drought when used in a similar fashion to our long-term trend analysis. Comparing the two simulations suggests that the temperature anomaly was responsible for −1.4 km^3 of the Millennium Drought runoff loss (total is −2.6 km^3), while the precipitation deficit caused −1.0 km^3 of the remaining −1.2 km^3 runoff loss. The average runoff in the P&T-detrend results is quite close to the long-term climatology (P&T-detrend: 18.7 km^3, climatology: 18.9 km^3, less than 1% difference), suggesting that the model precipitation and temperature changes are faithfully capturing the drought causes.

4. Interpretation and Discussion

4.1. Long-Term Trends

The Colorado River is snow-dominated, although only about 18% of the entire basin area accumulates enough SWE to produce substantial spring and summer RO (see 1 April SWE climatology >50 mm as shown in Figure 3c). Basin-wide 1 April SWE is approximately 20 km^3, which is close to the annual runoff at Lees Ferry. Li et al. (2017) show that for the UCRB, SWE accounts for 71% of annual runoff on average. Summer (April–September) RO constitutes almost ¾ of the total annual RO in both the UCRB and the entire basin. Clearly then, winter precipitation (and hence spring SWE) is closely linked to annual runoff changes. Although the overall winter precipitation trend from 1916 to 2014 is not significant over the entire UCRB (−0.2%, Table 2), uneven spatial distribution causes important winter precipitation decreases in several of the snow-dominant most runoff-productive headwater subbasins. Warming temperatures over our nearly hundred-year period of record in the UCRB (annual long-term ΔT is 1.8 °C as in Figure 2) induce −1.8 km^3 (53%) of the annual runoff losses totaling −3.4 km^3. The remaining −1.6 km^3 results from negative winter precipitation anomalies, mostly in the northeastern subbasins of UCRB (−1.0 km^3) and increasing winter ET (−0.6 km^3).

4.2. Winter ET and Sublimation

We found that increasing winter ET in both the baseline (4.9 km^3) and the T-detrend (2.9 km^3, Table 2) comes mainly from snow sublimation. In the T-detrend simulation, the November to February long-term change of UCRB sublimation is 2.2 km^3 (75.9% of the 2.9-km^3 ΔET$_{winter}$ increase) with the remaining 0.7 km^3 from increased evaporation in March. A possible cause of these trends in individual months was our approach using annual rather than seasonal (e.g., monthly) trend removal. Therefore, we performed another simulation with temperature detrended on a grid cell by grid cell basis for each month, instead of annually. This resulted in a considerable decrease in the March ET trend, which apparently was caused primarily by the increasing annual temperature trend. However, snow sublimation from October to February still showed increasing trends in this monthly T-detrend simulation. We were therefore left to explain the positive trends in snow sublimation over October–February given neither temperature nor precipitation trends.

We considered other factors that can influence the sublimation process in VIC. We found that the winter months had positive trends in surface aerodynamic resistance (AR), which leads to positive trend in surface snow sublimation. The AR trend was traced to the wind forcings in our VIC input data set, which are based on National Centers for Environmental Prediction /National Center for Atmospheric Research reanalysis, the record for which starts in 1949. Following Livneh et al. (2013), absent wind data prior to 1948, the earlier values were set to their monthly climatological averages. Although this approach did not result in a trend in wind over the 1916–2014 period, the nonlinear relationship between AR and wind speed results in larger AR values occurring after 1948 and thus results in the long-term increasing sublimation trend. While the resulting overall RO negative trend associated with this effect was modest (−0.6 km^3), we changed our pre-1949 wind values by randomly sampling from the later (post-1948) record. This resulted in the long-term UCRB annual RO trend becoming essentially zero in a new P&T detrend simulation. Livneh et al. (2013) reported that using wind climatology had only small impacts on their long-term mean RO, but in the case of the relatively dry CRB, the abrupt change in wind variability created artificial sublimation that was not negligible.

4.3. Drought Comparisons

Compared to the 1953–1968 drought, the causes of the Millennium Drought are more complicated. During the 1953–1968 drought, annual precipitation anomalies were negative across the entire CRB (Figure 8a) and temperature was close to its long-term mean (Figure 8b). Subbasin runoff anomalies, as well as SWE and ET anomalies, all responded primarily to the precipitation deficits. In contrast, the upper and lower parts of CRB behaved much differently during the Millennium Drought. In the UCRB, both winter and summer precipitation during 2000–2014 are just slightly below their climatologies (54.4 km³/winter compared to 55.8 km³/winter long-term mean) and 53.0 km³/summer (compared to 55.0 km³/summer long-term mean). The UCRB received approximately normal (slightly negative anomalies) winter precipitation, which was clearly higher than P_{winter} during 1953–1968 as noted in section 3.3, but produced less annual runoff (16.3 km³/yr versus 16.5 km³/yr).

The situation is reversed, however, if the temperature trend is removed. In this case the 1953–1968 drought becomes worse than the Millennium Drought. In the T-detrend simulation, the average annual runoff for the UCRB during 1953–1968 and 2000–2014 were 17.2 and 17.7 km³/yr, respectively (baseline annual runoff climatology is 18.9 km³). Therefore, the warming temperature accounts for 54% of the annual runoff anomaly during the Millennium Drought (−1.4 km³/yr of −2.6 km³/yr), which is very close to its 53% contribution to the long-term decreasing runoff trend. The other half of the runoff deficit was caused by UCRB's negative winter precipitation anomalies in the northeastern part of the basin where the highest runoff-generating subbasins are. The winter ΔP over 2000–2014 in those four highly productive subbasins was −2.4 km³/yr, much larger (in absolute value) than ΔP_{winter} over 1953–1968, −0.9 km³/yr. Exacerbated by above normal winter temperature in the baseline simulation, the UCRB winter ET anomaly over 2000–2014 was 1.8 km³/yr and ΔSWE is −4.4 km³/yr (23.7% less compared to the climatology).

These results demonstrate that warming temperature was a major driver for the UCRB's runoff shortage over the Millennium drought, in agreement with Udall and Overpeck (2017). In the Lower Basin, annual precipitation had very serious negative anomalies across the entire LCRB as shown in Figure 9a: all subbasins exhibited pronounced negative anomalies. While temperatures were also higher across the LCRB, there is no need to invoke a temperature forcing to explain the drought. As noted above, though, these LCRB precipitation anomalies have little effect on RO.

Using the Millennium Drought anomalies, we can estimate the runoff-precipitation-elasticity relationships as follows: the baseline average annual runoff for the UCRB is 18.9 km³, and the T-detrend runoff is 17.7 km³; therefore, the 1.2 km³ runoff decrease apparently is attributable to precipitation. Over 2000–2014 annual precipitation in the UCRB was 107.5 km³ and the climatology was 110.8 km³/yr, so ΔP/P is −0.029. The implied elasticity is 2.12 ($\Delta RO \cdot RO^{-1} \cdot \Delta P^{-1} \cdot P = -0.0616/-0.0291$), which is in good agreement with Vano et al. (2012).

4.4. Uncertainties

The results and analysis we have presented to this point are based on VIC simulations forced by the extended H&L data set. The robustness of the conclusions is potentially dependent on both the forcings and model performance. In order to examine the robustness of our results, we performed an exploratory uncertainty analysis of both the model forcings and hydrological model.

First, we compared the H&L forcings to two other widely used gridded climate datasets: Precipitation Regressions on Independent Slope Method (PRISM; Di Luzio et al., 2008) and Livneh (Livneh et al., 2013). Over the UCRB, trends in annual precipitation of these three data sets (H&L, PRISM, and Livneh) have long-term annual trends ranging from −6% to +2%, and for winter precipitation from −10% to +6%. As for the temperature, on an annual basis the positive trend over UCRB ranges from 1.0 °C to 1.4 °C and for winter temperature from 1.0 °C to 1.6 °C. As noted in the supporting information (Table S7), the H&L temperature trends generally are larger than for the other two data sets (also see section 2.1; the VIC temperature trend is not the same as the H&L trend but rather is somewhat larger, approximately 0.4 °C, as it results from energy budget closure in the model). The relatively large negative precipitation trend in Livneh is mostly attributable to large annual precipitation early in the record and in likelihood is traceable to the relatively liberal criterion that data set uses to allow entry of stations with relatively short record lengths.
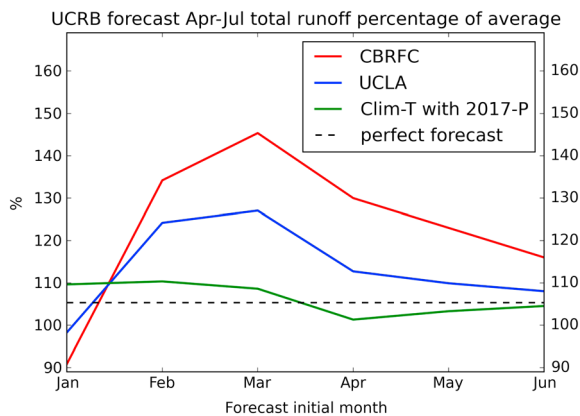
Figure 10. April–July 2017 streamflow forecasts at Lees Ferry initialized on the first day of each month expressed as percentages relative to 1981–2010 climatology. Red line represents the official forecasts published by CBRFC; blue line represents equivalent VIC reforecasts; green line is forecast with perfect precipitation forecast and temperature climatology. The horizontal dashed line is from a forecast with perfect precipitation and temperature.

Our choice of the H&L data set is based on its relationship with the HCN station data (to which its decadal variability is controlled; see Hamlet & Lettenmaier, 2005). The HCN data have been carefully quality controlled and in this sense arguably are more appropriate for trend-related studies than are the other two data sets (or for that matter, other data sets we might have chosen). We evaluated the H&L long-term temperature trend over UCRB (1.4 °C increase) in comparison with the simple average over all HCN stations in the UCRB (also 1.4 °C increase; identical to two significant figures). On this basis, and given the criteria used in construction of the H&L data set, we believe that it is most appropriate for our purposes. We do not believe that other methods that, for instance, might use multiple ensembles and effectively average either inputs to our outputs from our hydrological model would be appropriate given the objectives of our analysis.

As for hydrological models, we extracted the Noah-MP and VIC results from the UCLA Drought Monitor (Xiao et al., 2016) for model comparison (note that the forcings for the UCLA Drought Monitor are different than H&L but are common to the two models). Over the entire Upper Basin and the four most productive subbasins we identified, the long-term trends in Noah-MP and VIC runoff are generally consistent, for instance, for the entire UCRB (VIC: -3.5 km^3/yr; Noah-MP: -4.3 km^3/yr); see also subbasin trends shown in Figure S2. Although different models would no doubt produce somewhat different results, the fact that VIC and Noah-MP, which have essentially no common heritage, produce similar trends gives us some confidence that our results are reasonable model independent.

This uncertainty analysis improves the confidence in our conclusions. Nonetheless, more work could be done along these lines. For example, there is substantial uncertainty in the gridded forcing data sets we used, which are sparse and especially rare at high elevations. More sophisticated methods could be used to represent the uncertainty in the gridded data sets (aside from testing sensitivity to different data sets, as we have done). Furthermore, land surface models, which simulate complex systems, contain approximations and uncertainties that produce errors that are difficult to represent in analyses such as ours. Thus, given computational constraints, less than complete understanding of physical processes and limited observation resolutions, state-of-the-art land surface models will inevitably produce somewhat uncertain results. We acknowledge these uncertainties, which no doubt will motivate future work. We nonetheless argue that our results in the larger sense transcend the effects of these uncertainties, in particular given their robustness with respect to models and model forcing data sets.

5. The 2017 Streamflow Forecast

The Colorado Basin River Forecast Center (CBRFC) produces seasonal (April–July) streamflow forecasts starting about 1 January with monthly updates for the CRB using its Ensemble Streamflow Prediction (ESP) approach (Werner & Yeager, 2013) based on the Sacramento Soil Moisture Accounting model (Burnash et al., 1973). General characteristics of Sacramento and VIC simulations, and hence ESP forecasts, are roughly similar (Vano et al., 2012). The CBRFC forecast utilizes historical meteorological forcings for 1981–2010 to generate an ensemble of future streamflow series given hydrological conditions (soil moisture and SWE) on the forecast initiation date (e.g., 1 April), which are taken from a historical model simulation. We analyzed the forecasts issued on the first day of each month in 2017 from January to June. The official CRBFC forecast for the UCRB 2017 April–July streamflow (natural flow at Lees Ferry) decreased dramatically from much above normal on 1 January as the runoff season progressed. Some media reports attributed these decreases to anomalously warm late winter and spring conditions and drew parallels between water year 2017 conditions and the long-term trends analyzed above, especially in temperature.

We evaluated the causes of the changes in the 2017 forecasts using the same ESP approach as used by CRBFC but using the VIC rather than the Sacramento model. Because the ESP method requires near-real-time records and meteorological forcings, we used the UCLA/UW Drought Monitor data set (see Xiao et al., 2016) to perform the retrospective ensemble forecasts.
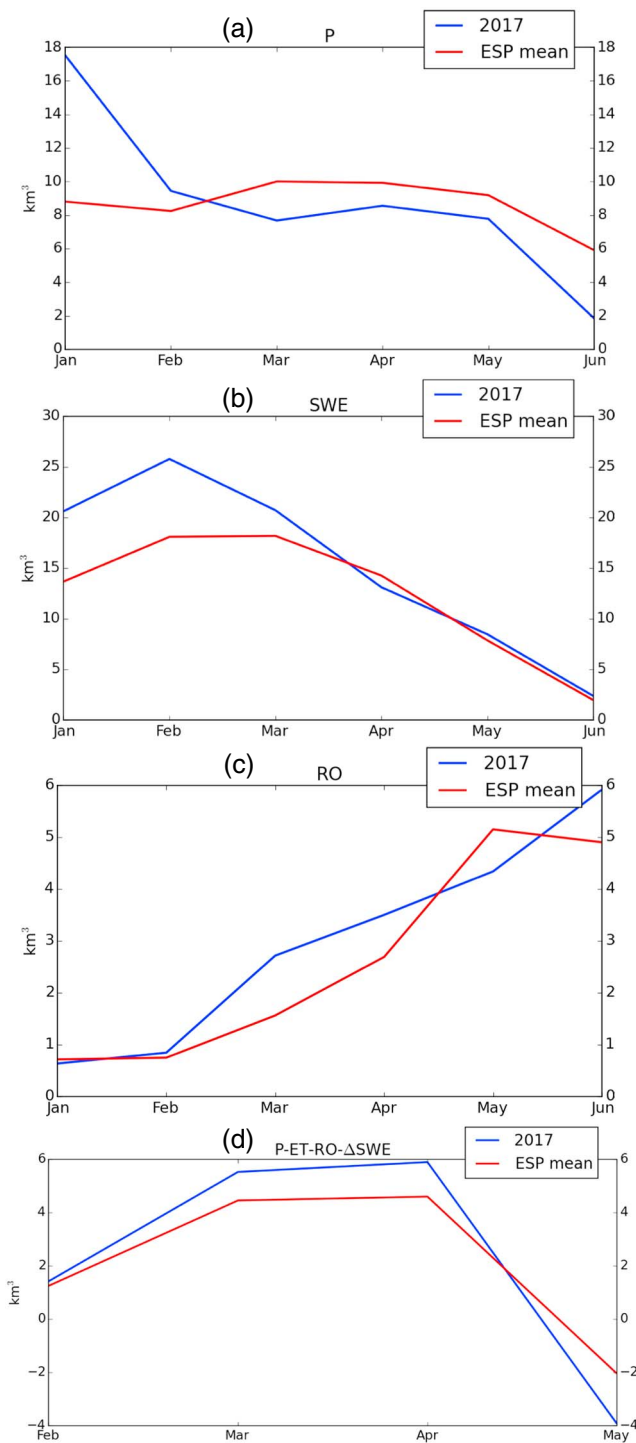
Figure 11. Monthly time series plots of (a) precipitation, (b) SWE, (c) runoff, and (d) soil moisture change. The blue line is the 2017 forecast; red line is historical climatology.

Figure 10 shows the predicted naturalized streamflow at Lees Ferry for each forecast initialized on the first day of each month. The red line shows the official forecasts produced by CRBFC, and the blue line is the average of the ensemble predictions generated using the UCLA/UW drought monitor data set. The green line shows the streamflow predictions that would have been made with a perfect precipitation forecast (they come from a VIC simulation with observed 2017 precipitation) but with temperature ensembles taken from observations for 1981–2010.

We performed this experiment to separate the effect of precipitation and temperature on the ESP results. In interpreting the forecasts, it is important to note that the forecast period is the same (April–July) for all forecasts, even though for post 1 April forecasts, part of the forecast period has already occurred, and some of the water literally has already gone *under the bridge*. It is clear that both the red and blue curves exhibit peaks around February–March with forecasts declining later. The CBRFC forecasts are higher than those made with VIC, which most likely is attributable to a different hydrologic model and different model forcing data sets; however, both sets of forecasts have the same general patterns. Also, both sets of forecasts are still above climatology for the last forecast (1 June), due to anomalously high SWE early in the forecast period. From the green line we can infer that the differences between the perfect precipitation forecasts initialized at each time and climatology are considerably smaller than the differences between either of the ESP forecast sets and climatology.

Given the perfect precipitation forecasts, the forecasts vary from 100% to 110% of the mean, which are close to the true value (observed flow relative to climatology) of 105.3%. Anomalously warm temperatures in February and March 2017 (plots are not shown here) caused some error in the forecasts: the streamflow forecasts initialized on 1 February and 1 March are both higher than observed because the climatology is cooler, but the differences are modest. In general, warm temperatures lead to less runoff and vice versa but this appears not to be the primary explanation for the rapid decrease in the two ESP ensemble means through the winter and early spring.

Figure 11 shows the monthly time series plots of precipitation, SWE, runoff, and soil moisture change (P-ΔSWE-ET-RO) for the UCRB for both 2017 and climatology from 1981 to 2010. The precipitation plot (Figure 11a) shows that the UCRB received anomalously high precipitation in January and February (with the highest anomaly in January), but the precipitation later in the forecast period was less than climatology. The direct effect is that in February 2017 there was a large positive SWE anomaly (Figure 11b), but the anomaly decreased thereafter. This explains why the ESP forecast peak was in February.

The RO time series plot in Figure 11c is more complicated: RO production was anomalously high in March, April, and June but lower than climatology in May. The question of interest is where did the snowpack that accumulated in January and February go? From Figure 11b, about 5 km³ of SWE melted in February and March. However, precipitation anomalies were in the range (negative) 2–4 km³ for each month from March 2017 on. The fact that 2017 ET during the forecast period was close to climatology (plot not shown) suggests that enhanced early season snowmelt supplied water to the soil column, but reduced subsequent precipitation hindered runoff production.

Figure 11d shows the modeled water balance for the soil column (P-ET-RO-ΔSWE). Figure 11d shows that ΔSMs in March and April are larger than climatology, but not by much. Furthermore, runoff generation

(Figure 11c) is above climatology during that period. However, as the precipitation deficit persisted into late spring and summer, SM began to decrease substantially. The RO actually produced was less than the early forecasts (initialized in February and March) because the ESP ensemble mean effectively corresponds to normal precipitation, which is higher than actually occurred from late winter on in 2017. In summary, the sharp reduction in forecasts through late winter and spring appears to be primarily related to negative anomalies in late winter precipitation, with anomalously warm late winter temperatures having a secondary effect.

6. Summary and Conclusions

Both long-term (~100 years) trends in streamflow and comparisons of two major drought periods (1953–1968 and Millennium) point to ongoing changes in the relative control of precipitation and temperature on the river's runoff. Udall and Overpeck (2017) have argued that a transition is occurring, which is especially evidenced by the different responses of the 1953–1968 and ongoing Millennium drought to precipitation and temperature anomalies. We find that while there is strong evidence for such a transition, the situation is complicated by spatial variations across the subbasins that contribute most to both long-term trends and drought variations in the basin, as well as to seasonal differences in temperature and precipitation trends and anomalies. Specifically, we conclude the following:

1. Over the UCRB (which produces about 90% of the entire basin's runoff), the long-term 1916–2014 decreasing trend of annual runoff is -3.4 km^3 (or -16.5% over the entire record). The increasing trend in annual temperature averaged over the basin over the same period has been 1.8 °C. When the annual temperature trend is removed, the negative trend in annual runoff becomes -1.6 km^3, which suggests that warming caused a little over half (1.8 km^3 or 53%) of the annual runoff trend. Four snow-dominated subbasins in the northeast part of the basin that in combination account for over half of the UCRB runoff have experienced modest declines in winter precipitation, which account for a substantial part of the UCRB runoff trend (-1.0 km^3) that is not attributable to warming. The remainder of the runoff loss (-0.6 km^3) is mostly associated with increased winter ET (mainly snow sublimation).

2. Compared to the 1953–1968 drought, which was caused by a basin-wide precipitation deficit, the Millennium Drought reflects a strong influence of warmer temperatures. The UCRB experienced low streamflow (2.6 km^3/yr below average, slightly more severe than the 2.4 km^3/yr negative anomaly for 1953–1968) during the Millennium Drought years (2000–2014 in our analysis). The four subbasins in the northeastern part of the UCRB with the largest negative long-term trends are also the major contributors to Millennium Drought runoff anomalies. The decrease of runoff for the Colorado River near Cameo was especially prominent—it alone accounts for over half of the 2000–2014 runoff anomalies. Although subbasins with positive runoff anomalies on the south side of Uinta Mountains such as the Duchesne and San Rafael Rivers counteract some of the deficit, UCRB Millennium Drought runoff was well below normal due primarily to deficits in the northeastern subbasins.

3. During the Millennium Drought years, the UCRB's precipitation was close but slightly below the long-term climatology (annual: 107.5 versus 110.8 km^3/yr; winter: 54.5 versus 55.8 km^3/yr). However, Millennium Drought annual precipitation was higher than the average for 1953–1968 (104.6 km^3/yr). Winter precipitation during the Millennium Drought was also higher than in the 1953–1968 drought; only summer precipitation was slightly lower. However, the highly productive subbasins in the northeastern portion of the UCRB had comparatively large winter precipitation deficits during 2000–2014, which resulted in 1.0 km^3/yr of the UCRB streamflow total reductions (2.6 km^3/yr) that were not attributable to warming. Warming temperatures caused 1.4-km^3/yr runoff losses.

4. By reforecasting the 2017 April–July natural streamflow at Lees Ferry using the same ESP approach used by CBRFC, we reproduce similar reductions in forecasted runoff to the CBREFC forecasts through the forecast season in what started as a large positive forecast anomaly in April–July runoff forecast on 1 January. The April–July forecast peaked around March 2017 due to abundant SWE in the UCRB induced by high early winter precipitation. Anomalously high snowmelt increased runoff in March and April. However, precipitation from March on continued below normal, and the forecast trended downward in the later months, eventually ending with only modestly above normal April–July runoffs. Anomalously warm temperatures from late winter on in 2017 aggravated the situation but appear not to be the major cause of the forecast declines, which rather was relatively dry conditions from midwinter on.

Given the importance of the Colorado River Basin to the rapidly growing U.S. Southwest, others likely will address the causes of the both the long-term and recent changes in CRB runoff, and the future implications of these findings as the 21st century continues to warm. As we noted in section 4.4, our results and conclusions are tightly linked with the forcing data set and the model (s) we used. The gridded forcings (for precipitation and temperature, as well as other variables derived from them) propagate through the hydrologic modeling and in turn our diagnosis of runoff changes. We opted to use the Hamlet and Lettenmaier (2005) forcing data set because it is closely linked to the U.S. Hydroclimatic Network (HCN; Easterling et al., 1996), which is based on a set of stations with relatively complete long-term records that have been corrected for station moves and instrument changes. Nonetheless, the stations included in HCN are predominantly at low elevations, and various avenues (e.g., assimilation of available surface and/or satellite observations into a coupled land/atmosphere model) could be pursued to better represent the role of high-elevation climatic changes, which may well not have occurred in concert with changes at lower elevations. We also note in section 4.4 (and explore, via limited experiments with a second model, Noah-MP) the possible sensitivity of our results to the form of the LSM, but much more could be done in this respect. Finally, we note that all of our experiments are offline; hence, we partition CRB runoff changes into those associated with warming temperatures and other factors (mostly precipitation changes); however, these multivariate changes may well be linked in ways that we have not explored. For instance, the modest changes in precipitation that we examined may be coupled with temperature changes and/or changes in the atmospheric radiative balance, and such linkages certainly are worth exploring.

References

Andreadis, K. M., Storck, P., & Lettenmaier, D. P. (2009). Modeling snow accumulation and ablation processes in forested environments. *Water Resources Research*, *45*, W05429. https://doi.org/10.1029/2008WR007042

Barnett, T. P., & Pierce, D. W. (2009). Sustainable water deliveries from the Colorado River in a changing climate. *Proceedings of the National Academy of Sciences of the United States of America*, *106*(18), 7334–7338. https://doi.org/10.1073/pnas.0812762106

Burnash, R. J. C., Ferral, R. L., & McGuire, R. A. (1973). A generalized streamflow simulation system—Conceptual modelling for digital computers (204 pp.).

Christensen, N. S., & Lettenmaier, D. P. (2007). A multimodel ensemble approach to assessment of climate change impacts on the hydrology and water resources of the Colorado River Basin. *Hydrology and Earth System Sciences Discussions*, *11*(4), 1417–1434. https://doi.org/10.5194/hess-11-1417-2007

Christensen, N. S., Wood, A. W., Voisin, N., Lettenmaier, D. P., & Palmer, R. N. (2004). The effects of climate change on the hydrology and water resources of the Colorado River basin. *Climatic Change*, *62*(1-3), 337–363. https://doi.org/10.1023/B:CLIM.0000013684.13621.1f

Cohen, M., Christian-Smith, J., & Berggren, J. (2013). Water to supply the land: Irrigated agriculture in the Colorado River Basin. Retrieved from http://water.usgs.gov/watercensus/colorado.html

Dawadi, S., & Ahmad, S. (2012). Changing climatic conditions in the Colorado River Basin: Implications for water resources management. *Journal of Hydrology*, *430-431*, 127–141. https://doi.org/10.1016/j.jhydrol.2012.02.010

Di Luzio, M., Johnson, G. L., Daly, C., Eischeid, J. K., & Arnold, J. G. (2008). Constructing retrospective gridded daily precipitation and temperature datasets for the conterminous United States. *Journal of Applied Meteorology and Climatology*, *47*(2), 475–497. https://doi.org/10.1175/2007JAMC1356.1

Easterling, D. R., Karl, T. R., Mason, E. H., Hughes, P. Y., & Bowman, D. P. (1996). United States Historical Climatology Network (US HCN), monthly temperature and precipitation data (280 pp.). http://cdiac.esd.ornl.gov/ndps/ushcn/abstract_r3.html

Hamlet, A. F., & Lettenmaier, D. P. (2005). Production of temporally consistent gridded precipitation and temperature fields for the continental United States. *Journal of Hydrometeorology*, *6*(3), 330–336. https://doi.org/10.1175/JHM420.1

Li, D., Wrzesien, M. L., Durand, M., Adam, J., & Lettenmaier, D. P. (2017). How much runoff originates as snow in the western United States, and how will that change in the future? *Geophysical Research Letters*, *44*, 6163–6172. https://doi.org/10.1002/2017GL073551

Liang, X., & D. Lettenmaier (1994). A simple hydrologically based model of land surface water and energy fluxes for general circulation models. *Journal of Geophysics*. *99*, 14,415–14,428. https://doi.org/10.1029/94JD00483/full (Accessed April 16, 2014).

Livneh, B., Rosenberg, E. A., Lin, C., Nijssen, B., Mishra, V., Andreadis, K. M., et al. (2013). A long-term hydrologically based dataset of land surface fluxes and states for the conterminous United States: Update and extensions. *Journal of Climate*, *26*(23), 9384–9392. https://doi.org/10.1175/JCLI-D-12-00508.1, http://journals.ametsoc.org/doi/abs/10.1175/JCLI-D-12-00508.1 (Accessed October 22, 2014).

McCabe, G. J., & Wolock, D. M. (2007). Warming may create substantial water supply shortages in the Colorado River basin. *Geophysical Research Letters*, *34*, L22708. https://doi.org/10.1029/2007GL031764

McCabe, G. J., Wolock, D. M., Pederson, G. T., Woodhouse, C. A., & McAfee, S. (2017). Evidence that recent warming is reducing upper Colorado river flows. *Earth Interactions*, *21*(10), 1–14. https://doi.org/10.1175/EI-D-17-0007.1

Mote, P. W., Hamlet, A. F., Clark, M. P., & Lettenmaier, D. P. (2005). Declining mountain snowpack in western North America. *Bulletin of the American Meteorological Society*, *86*(1), 39–50. https://doi.org/10.1175/BAMS-86-1-39

Mote, P. W., Li, S., Lettenmaier, D. P., Xiao, M., & Engel, R. (2018). Dramatic declines in snowpack in the western US. *npj Climate and Atmospheric Science*, *1*(1), 2. https://doi.org/10.1038/s41612-018-0012-1, http://www.nature.com/articles/s41612-018-0012-1

Prairie, J., & Callejo, R. (2005). Natural flow and salt computation methods, calendar years 1971-1995. Bureauof Reclamation, Salt Lake City, Utah and Boulder City, Nevad, Final, 1–112. Retrieved from http://digitalcommons.usu.edu/govdocs/135/%5Cnpapers2://publication/uuid/6183E843-86FF-4150-9535-C0407CB5477D

Rajagopalan, B., Nowak, K., Prairie, J., Hoerling, M., Harding, B., Barsugli, J., et al. (2009). Water supply risk on the Colorado River: Can management mitigate? *Water Resources Research*, *45*, W08201. https://doi.org/10.1029/2008WR007652

Reynolds, L. V., Shafroth, P. B., & LeRoy Poff, N. (2015). Modeled intermittency risk for small streams in the Upper Colorado River Basin under climate change. *Journal of Hydrology*, *523*, 768–780. https://doi.org/10.1016/j.jhydrol.2015.02.025

Rosenberg, E. A., Clark, E. A., Steinemann, A. C., & Lettenmaier, D. P. (2013). On the contribution of groundwater storage to interannual streamflow anomalies in the Colorado River basin. *Hydrology and Earth System Sciences*, *17*(4), 1475–1491. https://doi.org/10.5194/hess-17-1475-2013

Sen, P. K. (1968). Estimates of the regression coefficient based on Kendall' Stau Pranab Kumar Sen. *Journal of the American Statistical Association*, *63*(324), 1379–1389. https://doi.org/10.2307/2285891

Theil, H. (1950). A rank-invariant method of linear and polynomial regression analysis I. *NederlandseAkademie Wetenchappen*, *23*, 386–392. https://doi.org/10.1007/978-94-011-2546-8

U.S. Department of Interior, Bureau of Reclamation (1983). DRAFT Colorado River Simulation System Hydrology Data Base.

Udall, B., & Overpeck, J. (2017). The twenty-first century Colorado River hot drought and implications for the future. *Water Resources Research*, *53*, 2404–2418. https://doi.org/10.1002/2016WR019638

Vano, J. A., Das, T., & Lettenmaier, D. P. (2012). Hydrologic sensitivities of Colorado River runoff to changes in precipitation and temperature*. *Journal of Hydrometeorology*, *13*(3), 932–949. https://doi.org/10.1175/JHM-D-11-069.1

Vano, J. A., Udall, B., Cayan, D. R., Overpeck, J. T., Brekke, L. D., Das, T., et al. (2014). Understanding uncertainties in future Colorado River streamflow. *Bulletin of the American Meteorological Society*, *95*(1), 59–78. https://doi.org/10.1175/BAMS-D-12-00228.1

Werner, K., & Yeager, K. (2013). Challenges in forecasting the 2011 runoff season in the Colorado Basin. *Journal of Hydrometeorology*, *14*(4), 1364–1371. https://doi.org/10.1175/JHM-D-12-055.1

Woodhouse, C. A., Pederson, G. T., Morino, K., Mcafee, S. A., & Mccabe, G. J. (2016). Increasing influence of air temperature on upper Colorado River streamflow. 1–8. https://doi.org/10.1002/2015GL067613

Wu, H., Kimball, J. S., Li, H., Huang, M., Leung, L. R., & Adler, R. F. (2012). A new global river network database for macroscale hydrologic modeling. *Water Resources Research*, *48*, W09701. https://doi.org/10.1029/2012WR012313

Xiao, M., Nijssen, B., & Lettenmaier, D. P. (2016). Drought in the Pacific Northwest, 1920-2013. *Journal of Hydrometeorology*, *17*(9), 2391–2404. https://doi.org/10.1175/JHM-D-15-0142.1